Pré-Publicações do Departamento de Matemática
Universidade de Coimbra
Preprint Number 18–40

DRUG DELIVERY FROM BIMATERIAL ORTHOPEDIC IMPLANTS: A MATHEMATICAL APPROACH

RAQUEL BERNARDES, J.A. FERREIRA, M. GRASSI, M. NHANGUMBE AND PAULA DE OLIVEIRA

Abstract: The aim of this paper is to study a coupled model that describes drug release from a biodegradable polymeric surface, coated to a metallic device, and the evolution of a bacterial population adhering to the surface. Bacteria can cause infections, that are common events in orthopedic prosthesis, and are often responsible for rejection. A controlled drug delivery to fight bacterial adhesion is crucial in reducing infection rates. A strategy recently adopted to address the problem is to deliver therapeutic agents locally by dispersing them into polymeric implant coatings.

The mathematical model is composed by a system of three partial differential equations that describe the drug release from a biodegradable polymeric coating and by an ordinary differential equation that governs the density of a bacterial population. The link between the space-time differential system and the ordinary differential equation is defined by the mass of drug that is released by the polymeric structure at time t. Quasi-sharp estimates for the bacterial density, that give insight into its dependence on the polymeric properties and the drug characteristics, are established. Numerical experiments illustrating the behaviour of the density of bacteria, in function of the characteristics of the drug-polymeric coating system, are included.

Keywords: Drug release, biodegradable polymeric coating, PDE's system coupled with an ODE, sharp-estimates, numerical simulation.

1. Introduction

The main objective of this paper is to study the coupling of a system of partial differential equations (PDEs) of convection-diffusion-reaction type with an ordinary differential equation (ODE). The solution of the ODE depends on the solution of the PDE system and consequently indirectly it depends on the parameters that characterize the system. The motivation of the study is the modeling of the evolution of a bacterial population that develop on the surface of a medical implant and their evolution under the action of an antibacterial drug.

The drug is dispersed in a polymeric matrix that coats a metallic clinical device. When in contact with the interstitial fluid the drug is released to fight

Received October 2, 2018.

the threat of bacterial infections. The approach followed aimed at establishing theoretical estimates of the bacterial density with a sound physiological meaning. That is to say we look for solutions upper bounds sharp enough as to give relevant information about the behavior of the biotic population.

The following assumptions are considered to describe the physical, chemical and biological phenomena occurring in the surface of the drug eluting device:

(i) the polymer coating of a metallic device contains an antibacterial drug;
(ii) the interstitial fluid permeates the coating;
(iii) the polymer degrades in contact with the fluid, the chains broke and the drug is released;
(iv) the fluid molecules induce a dissolution process;
(v) the dissolved drug molecules diffuse through the polymeric platform and are released to the physiological environment;
(vi) the bacteria adhere to the surface of the polymeric coating in a "race for the surface", between host and pathogens.

As the fluid permeates the polymeric coating, the polymer swells and a pressure gradient arises. The swelling of the polymer is induced by a set of complex phenomena that occur in the polymeric chains and it requires that the partial differential equations are defined in a moving boundary domain. To simplify, we assume in what follows that the polymeric swelling is instantaneous and that all the phenomena occur after the swelling.

The model studied here contributes to highlight the dependence of the amount of drug released, on its own properties, the polymeric matrix properties and the characteristics of the particular bacterial population. We assume that the transport of the fluid is described by a convection-diffusion process in a porous medium. We also assume that the drug diffusion coefficient depends on the porosity, that increases with the degradation.

The drug is initially dispersed in the polymeric matrix and, as the fluid enters, a dissolution process takes place. We hypothesize that, when the release of drug starts, the corresponding polymeric structure is completely relaxed. Consequently we describe the delivery as a convection-diffusion-reaction process where the diffusion coefficient depends on the fluid concentration within the matrix and on the porosity. The tuning parameters of the drug release are the degradation rate of the polymeric matrix, the fluid diffusion coefficient, the drug diffusion coefficient, the rate of the interstitial fluid and the drug dissolution rate.

The drug release from the polymeric coating is coupled with an ordinary differential equation that governs the time evolution of a bacterial population density. The two differential problems are linked by the drug mass that is released at each time from the polymeric structure. The time evolution of the bacterial population is studied in function of the tuning parameters of the polymeric matrix and the drug.

The mathematical problem studied here can be used to simulate drug release from metallic clinical devices when the metal surface is coated with a biodegradable polymer where a drug is dispersed. Biocompatible metals and metallic alloys are extensively used in medical devices but, despite biocompatibility, infections occur as pathogens adhere to implant surfaces. We note that almost all implants, as for example coronary stents, catheters, pacemakers, valves, cochlear implants, breast implants and contact lenses, can be colonized by bacteria. Bacteria develop a biofilm where they are protected from the immune system and they gain resistance to antibiotics ([22]). In a simplified way, we will say that there is a "race for the surface", between host and pathogens which compete to determine the fate of the implant.

Infections related to orthopedic implants are the main cause of the failure of these devices. Such infections are caused by bacteria like *staphylococcus aureus*, *staphylococcus epidermis* that are often present in the operation room where they are harmless. Implant infections are extremely resistant to antibiotics and host defenses. Several strategies have been explored to control infections and other adverse tissue reactions, as inflammation or rejection. Systemic administration of drugs leads to a relatively low drug concentration at the target site and the administration of higher concentrations may only increase the occurrence of side effects as toxicity, renal and liver complications.

Efficient ways of delivering drug through *in situ* clinical eluting devices are desirable and this has given rise to several approaches. The mixing of drug and bone cement represents a precursor of local drug delivery in orthopedy. However, in real systems the drug mainly diffuses through the cracks that are formed during the cement drying process. This means that it is difficult to control the release rate. Also adding the antibiotic decreases the material's durability, leading to an high incidence of bone cement fractures [24].

The use of metallic prosthesis offered new types of solutions. For example, in [17], the authors proposed a hollow titanium implant perforated with microholes loaded with drug and showed that a release of the drug up to

7 weeks was observed. In [7], a stainless steel hollow tubular reservoir with encapsulated drug has been proposed for fixation pins used in orthopedic applications. The coating of metallic prosthesis with polymeric materials, where drug has been dispersed, has generated much interest during the last years [2, 6, 8, 14, 16, 24, 25, 26]. Recently, researchers of the Massachusetts General Hospital published a paper [24], in Nature, where they proposed a drug eluting polymeric implant that maintains the necessary mechanical strength.

To move a step forward in the field, mathematical models of drug delivery from polymeric coatings of metallic devices can be of great help to manufacturers and clinicians. First of all the influence of mechanical properties can be tested. This point has been largely studied in the literature (see for instance [18, 26] and their references) and will not be addressed in the present paper. Secondly the behavior of drug release can be simulated for short and long times. Both behaviors have clinical importance: early times - the first 6 hours [20] after surgery - are crucial to prevent pathogens from rapid proliferation; late times act as long time defense. Therefore, variable sequential drug delivery systems with several distinctly different release profiles have been developed [23].

In previous works of some of the authors, models of drug release from polymeric platforms and applications to drug eluting stents have been presented (see for instance [3, 4, 5, 15]). From a theoretical point of view, the originality of the present paper stands on the type of coupling between the drug delivery from the polymeric matrix and the time evolution of the density of bacteria. The approach followed leads to stability estimates of the population density that depend on the properties of the release platform. These estimates, based on functional arguments are needed to prove stability and existence results. However they also show how to bridge the gap between the theoretical analysis of a model and its practical outcomes. In fact they represent a contribution that can be used to assist in tuning drug delivery from a medical device and its effect on opportunistic bacterial populations.
In Section 2 we present the mathematical model. In Section 3 we establish a number of stability results. Numerical simulations are presented in Section 4 and finally, in Section 5 some conclusions are included.

2. Drug release from a polymeric coating

2.1. Mathematical model. We consider a simplified geometry for the drug release system: it is composed by a metallic cube with a biodegradable polymeric coating on its top (see Figure 1a)). A drug in the solid state is initially dispersed in the polymeric coating. To simulate the behaviour of the delivery system *in vitro*, we assume that the device is inside of a Petri dish containing a solvent. This geometry simulates for instance the behaviour of a sample of a bimaterial orthopedic implant composed by a metallic platform and a polymeric coating. We assume that the polymeric coating with the dispersed drug is an isotropic medium. This fact allows us to replace the 3D geometry by a 2D computational domain (see Figure 1b)) defined by the intersection of the 3D solid with a plan.

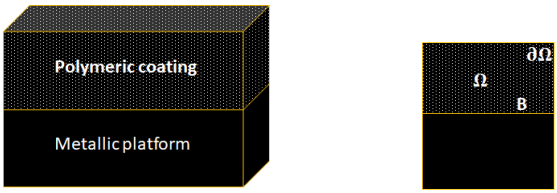

a) b)

FIGURE 1. a) 3D Metallic structure and the polymeric coating imbedded in a fluid b) The computational domain Ω imbedded in the fluid.

Let Ω denote the spatial domain represented in Figure 1b) and let T be a fixed time. By $c_\ell(x, y, t)$ we represent the fluid concentration in $(x, y) \in \overline{\Omega}$ at time t. The fluid, in contact with the polymeric coating, permeates the matrix and is absorbed due to a concentration gradient. Moreover, the polymeric coating swells and a pressure gradient arises that induces a convective transport. To make the model more intelligible, we assume that swelling is instantaneous and that the viscoelastic properties of the polymeric matrix have no influence on the release process.

To simplify the presentation, if $w : \overline{\Omega} \times [0, T] \to \mathbb{R}$, then by $w(t)$ we denote the following function $w(t) : \overline{\Omega} \to \mathbb{R}$ such that $w(t)(x, y) = w(x, y, t), (x, y) \in \overline{\Omega}$.

Let $J_\ell(t)$ be the fluid mass flux. Then

$$J_\ell(t) = -D_\ell(t)\nabla c_\ell(t) + v c_\ell(t) \quad \text{in } \Omega \times (0, T], \tag{1}$$

where, v stands for the fluid velocity and $D_\ell(t)$ the liquid diffusion coefficient. Neglecting the gravitational force, $v(t)$ is given by Darcy's law

$$v = -\frac{k}{\mu}\nabla p \ \text{ in } \Omega, \tag{2}$$

where p denotes the fluid pressure, k and μ denote the permeability and the fluid viscosity coefficients, respectively. As the fluid is incompressible, equation (2) is coupled with

$$\nabla.v = 0 \text{ in } \Omega. \tag{3}$$

To keep the mathematical problem analytically manageable, we assume that the velocity is known ([11]).
The release of the dissolved drug from the biodegradable polymeric coating depends on polymer degradation, drug diffusion and convective transport. As the polymeric coating degrades in the presence of the fluid, its porosity increases, altering the diffusion and convective transports. We assume that the liquid diffusion coefficient $D_\ell(t)$ satisfies

$$D_\ell(t) = \frac{\epsilon(t)}{\tau(t)} D_{\ell,0},$$

where $\epsilon(t)$ and $\tau(t)$ denote the porosity and the tortuosity coefficients, respectively, and $D_{\ell,0}$ represents the diffusion coefficient in the non-hydrolyzed polymer. As we assume that $\tau(t) = \epsilon(t)^{-1/2}(t)$, then

$$D_\ell(t) = \epsilon(t)^{3/2} D_{\ell,0}, \tag{4}$$

(see [19]).
Summing up the concentration $c_\ell(t)$ is solution of the following parabolic equation

$$\frac{\partial c_\ell}{\partial t} + \nabla.(vc_\ell) = \nabla.(D_\ell \nabla c_\ell) \text{ in } \Omega \times (0, T]. \tag{5}$$

Let $c_s(x, y, t)$ and $c_d(x, y, t)$ represent the solid and dissolved drug concentrations in $(x, y) \in \bar{\Omega}$ at time t, respectively. The kinetics of these two

unknown concentrations is described by the following system of partial differential equations

$$\begin{cases} \dfrac{\partial c_d}{\partial t}(t) + \nabla.(vc_d(t)) = \nabla.(D_{eff}(t)\nabla c_s(t)) + f(c_s(t), c_d(t), c_\ell(t)) \\ \\ \dfrac{\partial c_s}{\partial t}(t) = -f(c_s(t), c_d(t), c_\ell(t)), \quad \text{in}\,\Omega \times (0, T], \end{cases} \tag{6}$$

with

$$D_{eff}(t) = \frac{(1-\epsilon(t))D_1 + \tilde{k}\epsilon(t)D_2}{1-\epsilon(t)+\tilde{k}\epsilon(t)}, \tag{7}$$

where D_1 denotes the diffusion coefficient of the drug in the solid polymer and D_2 is the drug diffusivity in the liquid filled pores ([27]) . In (7), $\tilde{k}$ denotes the drug partition coefficient between the liquid pores and the solid polymer. In order to simplify, we take $\tilde{k} = 1$.
In [27], a mathematical model for drug release from PLGA (poly(D,L-lactic-co-glycolic acid) was established for cardiovascular drug delivery. In this model the authors assumed that the drug diffusion coefficient is defined by (7) with the porosity $\epsilon(t)$ given by

$$\epsilon(t) = \epsilon_0 + (1-\epsilon_0)(1 + e^{-2k_d t} - 2e^{-k_d t}), \tag{8}$$

where ϵ_0 represents the initial porosity coefficient and k_d denotes the polymeric degradation rate.
Following [27], we consider $\epsilon(t)$ defined by (8), D_{eff} given by (7), constant diffusion coefficients $D_i, i = 1, 2$, with $D_2 > D_1$.
A common choice for the function f that defines the kinetics of the undissolved and dissolved drugs is the following Noyes–Whitney relation

$$f(c_s(t), c_d(t), c_\ell(t)) = \alpha H(c_s(t))\frac{c_{sol} - c_d(t)}{c_{sol}}c_\ell(t), \tag{9}$$

where $H(.)$ denotes the Heaviside function, α the dissolution constant rate of the solid drug and c_{sol} the drug solubility (see for instance [10], [21]). However, when c_d is far from c_{sol}, it is appropriate to replace (9) by

$$f(c_s(t), c_d(t), c_\ell(t)) = \alpha H(c_s(t))\frac{c_s(t) - c_d(t)}{c_s(t)}c_\ell(t), \tag{10}$$

(see [3],[5]). If large solid drug particles are used then the total contact surface area, between drug and fluid, is smaller than in the case of small particles. As a consequence equation, (10) can be considered an accurate

description of the dissolution process if large drug particles are considered. In [13] the first order models

$$f(c_s(t), c_d(t), c_\ell(t)) = \alpha c_s(t),$$

and

$$f(c_s(t), c_d(t), c_\ell(t)) = k_1 c_s(t) - k_2 c_d(t),$$

are used with K_1, K_2 constants, however the role of the fluid concentration is not taken into account.

Synthesizing, the differential system that governs the release of drug is composed by: equation (5) for $c_\ell(t)$, with the diffusion coefficient of the fluid $D_\ell(t)$ given by (4) and the porosity $\epsilon(t)$ defined by (8); equation (6) for $c_d(t)$ and $c_s(t)$, with $D_{eff}(t)$ given by (7), $\tilde{k} = 1$, $D_i, i = 1, 2$, constant, and f given by (10).

To close the differential system we impose boundary, interface and initial conditions. We consider that the interface between the metallic structure and the polymeric coating is isolated (see Figure 1b); regarding the fluid that permeates through $\partial\Omega - B$, we assume that the incoming fluid depends on the polymer permeability β, that is

$$\begin{aligned} &J_\ell(t).\eta = 0 \text{ on } B, \\ &J_\ell(t).\eta = \beta(c_\ell(t) - c_{ext}) \text{ on } \partial\Omega - B, \end{aligned} \tag{11}$$

where c_{ext} denotes the exterior fluid concentration, η is the exterior unitary normal to Ω and $J_\ell(t)$ defined in (1).

For the dissolved drug $c_d(t)$ we assume that the drug molecules that reach $\partial\Omega - B$ are immediately absorbed by the exterior medium and that B is an isolated interface. These assumptions are represented by

$$\begin{aligned} &c_d(t) = 0 \text{ on } \partial\Omega - B, \\ &J_d(t).\eta = 0 \text{ on } B, \end{aligned} \tag{12}$$

where $J_d(t) = -D_{eff}\nabla c_d(t) + v c_d(t)$.

The initial conditions are defined by

$$c_s(0) = c_0,\ c_d(0) = 0,\ c_\ell(0) = 0 \text{ in } \Omega. \tag{13}$$

We observe that if the velocity is described by (2), (3) these equations should be complemented by the boundary conditions

$$v.\eta = 0 \text{ on } B, p = p_0 \text{ on } \partial\Omega - B, \tag{14}$$

where η denotes the exterior unitary normal at B.

2.2. Qualitative behaviour: quasi-sharp estimates. We start by establishing an upper bound for the total drug mass $M_d(t)$ in Ω

$$M_d(t) = \int_\Omega \big(c_d(t) + c_s(t)\big) d\omega.$$

As

$$\frac{\partial c_d}{\partial t}(t) + \frac{\partial c_s}{\partial t}(t) = -\nabla . J_d(t),$$

we successively deduce

$$\begin{aligned} M_d'(t) &= -\int_\Omega \nabla . J_d(t) d\omega \\ &= -\int_{\partial\Omega - B} J_d(t).\eta ds, \end{aligned}$$

where η is the exterior unitary normal. Considering the phenomenological ansatz $J_d(t).\eta > 0$, we conclude that

$$M_d'(t) \leq 0,\ t > 0,$$

and consequently

$$M_d(t) \leq M_d(0),\ t \geq 0,$$

which is physically acceptable.
In what follows we establish an estimate for the energy functional

$$E(t) = \|c_d(t)\|^2_{L^2(\Omega)} + \|c_s(t)\|^2_{L^2(\Omega)}, t \geq 0, \tag{15}$$

where $\|.\|_{L^2(\Omega)}$ denotes the usual norm in $L^2(\Omega)$ that is induced by the usual inner product $(.,.)_{L^2(\Omega)}$.

Let

$$H^1_{\partial\Omega - B,0}(\Omega) = \{u \in H^1(\Omega) : u = 0 \text{ on } \partial\Omega - B\}.$$

As $c_d(t) \in H^1_{\partial\Omega - B,0}(\Omega)$, there exists a positive constant C_P such that

$$\|c_d(t)\|_{L^2(\Omega)} \leq C_P \|\nabla c_d(t)\|_{L^2(\Omega)\times L^2(\Omega)}. \tag{16}$$

Inequality (16) is usually known as Friedrichs-Poincaré inequality. In this inequality, $L^2(\Omega) \times L^2(\Omega)$ represents the usual cartesian product of $L^2(\Omega)$ by itself and $\|.\|_{L^2(\Omega)\times L^2(\Omega)}$ denotes the usual norm in this space.

We establish now a two technical propositions that will be used in the study of the behaviour of the energy $E(t)$. By $\|.\|_\infty$ we represent the usual norm in $L^\infty(\Omega) \times L^\infty(\Omega)$, that is

$$\|w\|_\infty = \max_{i=1,2}\{ess\sup_\Omega |w_i|,\ w=(w_1,w_2)\in L^\infty(\Omega)\times L^\infty(\Omega)\}.$$

Proposition 1. *Let us suppose that the transport of the dissolved drug c_d is diffusion dominated in the sense that*

$$D_{eff}(t) - \|v\|_\infty C_P > 0. \tag{17}$$

If

$$\mu_\pm(t) = \frac{1}{\|v\|_\infty}\sqrt{D_{eff}(t) \pm \sqrt{D_{eff}(t)^2 - C_P^2\|v(t)\|_\infty^2}}, \tag{18}$$

then for $\mu \in]\mu_-(t), \mu_+(t)[$, where $\mu_\pm(t) > 0$, we have

$$\frac{1}{C_P^2}\Big(- D_{eff}(t) + \frac{1}{2}\|v(t)\|_\infty^2\mu^2\Big) + \frac{1}{2\mu^2} < 0, \tag{19}$$

$$D_{eff}(t) - \frac{1}{2}\|v\|_\infty^2\mu_\pm(t)^2 > 0 \tag{20}$$

Furthermore, for $\mu \in]\mu_-(0), \mu_+(0)[$, with

$$\mu_\pm(0) = \frac{1}{\|v\|_\infty}\sqrt{D_{eff}(0) \pm \sqrt{D_{eff}(0)^2 - \|v\|_\infty^2 C_P^2}}, \quad D_{eff}(0) = D_1 + \epsilon_0(D_2 - D_1),$$

we have (19), for all $t \geq 0$.

Proposition 2. *The function*

$$g(\mu) = \frac{1}{C_P^2}\Big(D_{eff}(0) - \frac{1}{2}\|v\|_\infty^2\mu^2\Big) - \frac{1}{2\mu^2},\ \mu \in]\mu_-(0), \mu_+(0)[,$$

attains its maximum at $\bar\mu = \sqrt{\dfrac{C_P}{\|v\|_\infty}} \in]\mu_-(0), \mu_+(0)[$ and, under assumption (17), we have

$$g(\bar\mu) = \frac{1}{C_P^2}\Big(D_{eff}(0) - \|v\|_\infty C_P\Big) > 0.$$

Moreover, for $\sigma^2 \in I(\sigma^2)$, with

$$I(\sigma^2) =]\frac{\bar\alpha C_P^2}{\bar\alpha C_P^2 + D_{eff}(0) - \|v\|_\infty C_P}, 1[, \tag{21}$$

$$\frac{1}{C_P^2}\Big(D_{eff}(0) - \|v\|_\infty C_P\Big) - \bar\alpha(\frac{1}{\sigma^2} - 1) > 0. \tag{22}$$

(**Proof:** See Appendix)

Let us now estimate $E(t)$. For the concentrations of fluid, $c_\ell(t)$, dissolved drug, $c_d(t)$, and solid drug $c_s(t)$, we obtain

$$\begin{aligned}(\frac{\partial c_\ell}{\partial t},\phi)_{L^2(\Omega)} &= -(D_\ell(t)\nabla c_\ell(t),\nabla\phi)_{L^2(\Omega)\times L^2(\Omega)} - (c_\ell(t)v,\nabla\phi)_{L^2(\Omega)\times L^2(\Omega)}\\ &\quad -\beta(c_\ell(t),\phi)_{L^2(\partial\Omega-B)},\ \forall\phi\in H^1(\Omega),\end{aligned} \tag{23}$$

where $(.,.)_{L^2(\partial\Omega-B)}$ denotes the usual inner product in $L^2(\partial\Omega-B)$,

$$\begin{aligned}(\frac{\partial c_d}{\partial t},\psi)_{L^2(\Omega)} &= -(D_{eff}(t)\nabla c_d(t),\nabla\psi)_{L^2(\Omega)\times L^2(\Omega)} - (c_s(t)v,\nabla\psi)_{L^2(\Omega)\times L^2(\Omega)}\\ &\quad +(f(c_s(t),c_d(t),c_\ell(t)),\psi)_{L^2(\Omega)},\ \forall\psi\in H^1_{\partial\Omega-B}(\Omega),\end{aligned} \tag{24}$$

where f is defined by (10), and

$$(\frac{\partial c_s}{\partial t},\omega)_{L^2(\Omega)} = -(f(c_s(t),c_d(t),c_\ell(t)),\omega)_{L^2(\Omega)},\ \forall\omega\in L^2(\Omega). \tag{25}$$

In Proposition 3 we establish an upper bound for the energy $E(t)$ defined by (15).

Proposition 3. *Let us suppose that the transport of the dissolved drug c_d is diffusion dominated in the sense that (17) holds and the fluid is in equilibrium that is $c_\ell(t)=c_{\ell,eq}$. Then*

$$E(t)\le e^{-Qt}\|c_s(0)\|^2_{L^2(\Omega)},\ t\ge 0, \tag{26}$$

where

$$Q=\frac{\bar\alpha(D_{eff}(0)-\|v\|_\infty C_P)}{\bar\alpha C_P^2+D_{eff}(0)-\|v\|_\infty C_P} \tag{27}$$

and

$$\bar\alpha=\frac{\alpha c_{\ell,eq}}{\|c_s(0)\|_\infty}. \tag{28}$$

Proof: Considering in (24) and (25) $\psi=c_d(t)$ and $\omega=c_s(t)$, respectively, we easily get

$$\begin{aligned}\frac{1}{2}E'(t) &= -(\alpha\frac{H(c_s(t))}{c_s(t)}c_{\ell,eq}(c_s(t)-c_d(t)),c_s(t)-c_d(t))_{L^2(\Omega)}\\ &\quad -(D_{eff}(t)\nabla c_d(t),\nabla c_d(t))_{L^2(\Omega)\times L^2(\Omega)} - (c_d(t)v,\nabla c_d)_{L^2(\Omega)\times L^2(\Omega)}.\end{aligned}$$

If we assume now that $c_\ell(t)$ is in equilibrium, then

$$\begin{aligned}\frac{1}{2}E'(t) \ &\leq \bar{\alpha}\Big(- \|c_s(t)\|^2_{L^2(\Omega)} - \|c_d(t)\|^2_{L^2(\Omega)} + 2(c_s(t), c_d(t))_{L^2(\Omega)}\Big) \\ &\quad -D_{eff}(t)\|\nabla c_d(t)\|^2_{L^2(\Omega)\times L^2(\Omega)} - (c_d(t)v, \nabla c_d(t))_{L^2(\Omega)\times L^2(\Omega)}.\end{aligned} \tag{29}$$

As for all $\mu \neq 0$ and $\sigma \neq 0$, we have

$$-(c_d(t)v, \nabla c_d)_{L^2(\Omega)\times L^2(\Omega)} \leq \frac{1}{2}\|v\|^2_\infty \mu^2 \|\nabla c_d(t)\|^2_{L^2(\Omega)\times L^2(\Omega)} + \frac{1}{2\mu^2}\|c_d(t)\|^2_{L^2(\Omega)} \tag{30}$$

and

$$2(c_s(t), c_d(t))_{L^2(\Omega)} \leq \sigma^2 \|c_s(t)\|^2_{L^2(\Omega)} + \frac{1}{\sigma^2}\|c_d(t)\|^2_{L^2(\Omega)},$$

from (29) we conclude

$$\begin{aligned}\frac{1}{2}E'(t) \ &\leq \bar{\alpha}\Big((\sigma^2 - 1)\|c_s(t)\|^2_{L^2(\Omega)} + (\frac{1}{\sigma^2} - 1)\|c_d(t)\|^2_{L^2(\Omega)}\Big) \\ &\quad +\Big(- D_{eff}(t) + \tfrac{1}{2}\|v\|^2_\infty \mu^2\Big)\|\nabla c_d(t)\|^2_{L^2(\Omega)\times L^2(\Omega)} + \tfrac{1}{2\mu^2}\|c_d(t)\|^2_{L^2(\Omega)}.\end{aligned} \tag{31}$$

Proposition 1 allows to conclude that (19) holds, for $\mu \in]\mu_-(t), \mu_+(t)[$, and then, using the Friedrichs-Poincaré inequality, we establish

$$\begin{aligned}\frac{1}{2}E'(t) \ &\leq \bar{\alpha}\Big((\sigma^2 - 1)\|c_s(t)\|^2_{L^2(\Omega)} + (\frac{1}{\sigma^2} - 1)\|c_d(t)\|^2_{L^2(\Omega)}\Big) \\ &\quad +\Big(\tfrac{1}{C_P^2}\Big(- D_{eff}(t) + \tfrac{1}{2}\|v\|^2_\infty \mu^2\Big) + \tfrac{1}{2\mu^2}\Big)\|c_d(t)\|^2_{L^2(\Omega)}.\end{aligned} \tag{32}$$

Moreover, as $D_{eff}(t)$ is an increasing function, then, for $\mu \in]\mu_-(0), \mu_+(0)[$, we also have

$$\begin{aligned}\frac{1}{2}E'(t) \ &+\Big(\tfrac{1}{C_P^2}\Big(D_{eff}(0) - \tfrac{1}{2}\|v\|^2_\infty \mu^2\Big) - \tfrac{1}{2\mu^2} - \bar{\alpha}(\tfrac{1}{\sigma^2} - 1)\Big)\|c_d(t)\|^2_{L^2(\Omega)} \\ &+\bar{\alpha}(1 - \sigma^2)\|c_s(t)\|^2_{L^2(\Omega)} \leq 0, \ t > 0.\end{aligned} \tag{33}$$

We choose now $\bar{\mu} \in]\mu_-(0), \mu_+(0)[$ that maximizes the coefficient of $\|c_d(t)\|^2_{L^2(\Omega)}$ in (33). From Proposition 2 we conclude that

$$\frac{1}{2}E'(t) + T_1(\sigma^2)\|c_d(t)\|^2_{L^2(\Omega)} + T_2(\sigma^2)\|c_s(t)\|^2_{L^2(\Omega)} \leq 0, \ t > 0, \tag{34}$$

where

$$T_1(\sigma^2) = \frac{1}{C_P^2}\Big(D_{eff}(0) - \|v\|_\infty C_P\Big) - \bar{\alpha}(\frac{1}{\sigma^2} - 1)\Big)$$

and

$$T_2(\sigma^2) = \bar{\alpha}(1 - \sigma^2).$$

From Proposition 2 we conclude that, for all $\sigma^2 \in I(\sigma^2)$, where $I(\sigma^2)$ is defined by (21), both the coefficients of $\|c_s(t)\|^2_{L^2(\Omega)}$ and $\|c_d(t)\|^2_{L^2(\Omega)}$ in (34) are positive.
We fix now $\bar{\sigma}^2$ as the midpoint of the interval $I(\sigma^2)$, that is

$$\bar{\sigma}^2 = \frac{\bar{\alpha}C_P^2 + \frac{1}{2}(D_{eff}(0) - \|v\|_\infty C_P)}{\bar{\alpha}C_P^2 + (D_{eff}(0) - \|v\|_\infty C_P)}.$$

Then

$$T_1(\bar{\sigma}^2) = \frac{(D_{eff}(0) - \|v\|_\infty C_P)(\bar{\alpha}C_P^2 + D_{eff}(0) - \|v\|_\infty C_P)}{C_P^2(2\bar{\alpha}C_P^2 + D_{eff}(0) - \|v\|_\infty C_P)}$$

$$T_2(\bar{\sigma}^2) = \frac{1}{2}\frac{\bar{\alpha}(D_{eff}(0) - \|v\|_\infty C_P)}{\bar{\alpha}C_P^2 + D_{eff}(0) - \|v\|_\infty C_P}.$$

As

$$T_1(\bar{\sigma}^2) \geq T_2(\bar{\sigma}^2),$$

from (34) we deduce

$$E'(t) + 2T_2((\bar{\sigma}^2)E(t) \leq 0,\, t > 0, \tag{35}$$

that leads to (26). ■

Corollary 1. *Under the assumptions of Proposition 3, the dissolved drug mass $M_d(t)$ satisfies*

$$M_d(t) \leq \sqrt{2|\Omega|}e^{-\frac{1}{2}Qt}\|c_s(0)\|_{L^2(\Omega)}, t \geq 0, \tag{36}$$

where Q is defined by (27) and $|\Omega|$ represents the measure of Ω.

To interpret (36) for practical outcomes, we analyze the behavior of Q ((27)) as a function of parameters $\bar{\alpha}$, ((28)), $D_{eff}(0)$, ((7)), $\|v\|_\infty$ and C_P ((16)). The results obtained are summarized in Table 1. We remark that C_P depends on the measure of the domain Ω and increases when Ω increases.
We conclude that estimate (36) is "quasi-sharp". Its behaviour is physical with parameters $D_{eff}(0), C_P, \bar{\alpha}, \epsilon_0$. The estimate can be considered sharp, regarding these parameters, because it gives insight on the type of functional dependence of $M_d(t)$. An exception arises for $\|v\|_\infty$. This lack of sharpness could be expected because in (30) we replaced $-(c_d(t)v, \nabla c_d(t))_{L^2(\Omega)\times L^2(\Omega)}$ by a term that is always positive.

Partial derivative	Sign	Monotony of the upper bound of $M_d(t)$	Previewed behaviour of $M_d(t)$
$\frac{\partial Q}{\partial D_{eff}(0)}$	$+$	Decreases with $D_{eff}(0)$	Physical
$\frac{\partial Q}{\partial C_P}$	$-$	Increases with C_P	Physical
$\frac{\partial Q}{\partial \bar{\alpha}}$	$+$	Decreases with $\bar{\alpha}$	Physical
$\frac{\partial Q}{\partial \|v\|_\infty}$	$-$	Increases with $\|v\|_\infty$	Non physical
$\frac{\partial Q}{\partial \epsilon_0}$	$+$	Decreases with ϵ_0	Physical

TABLE 1. Dependence of drug mass on the parameters of the model

3. Time evolution of the concentration of bacteria

In what follows we consider the coupling of the drug release problem (5), (6), (11), (12), (13) with an ordinary differential equation that describes the evolution of a population of pathogens under the action of the drug. Let $N(t)$ represent the population density. We consider the equation

$$\frac{dN}{dt}(t) = \Big(\lambda - F(M_s(t))\Big)N(t), t > 0, \tag{37}$$

where $M_s(t)$ is the drug mass released at time t through $\partial\Omega - B$

$$M_s(t) = \int_{\partial\Omega - B} J_d(t).\eta ds \tag{38}$$

and

$$F(y) = \frac{E_{max}y^\gamma}{M_{50}^\gamma + y^\gamma} \tag{39}$$

with E_{max}, M_{50} and γ constants.
Equation (37) is obtained from Hill model ([9])

$$\frac{dN}{dt}(t) = \Big(\lambda - \frac{E_{max}c_d(t)^\gamma}{c_{50}^\gamma + c_d(t)^\gamma}\Big)N(t),\ t > 0, \tag{40}$$

that is used to describe the evolution of bacteria under the action of an antibacterial agent with concentration $c_d(t)$. The Hill model is extensively used in the literature and probably one of the reasons for its success is its flexibility and effectiveness in fitting experimental data ([9]).

In (40), $N(t)$ denotes the bacterial density, λ is the growth rate of bacteria, E_{max} denotes the maximum drug effect, c_{50} is the drug concentration producing 50% of the maximum effect and γ represents a measure of the cooperation between bacteria. If $\gamma = 1$ the adhesion of the bacteria to the surfaces is independent of each other; if $\gamma > 1$, then there is cooperation; if $\gamma < 1$ no cooperation occurs.
If V_{bio} denotes the volume of the bacterial habitat then

$$\begin{aligned} F(c_d(t)) &= \frac{E_{max}(V_{bio}c_d(t))^\gamma}{(V_{bio}c_{50})^\gamma + (V_{bio}c_d(t))^\gamma} \\ &= \frac{E_{max}M_{bio}(t)^\gamma}{(V_{bio}c_{50})^\gamma + M_{bio}(t)^\gamma}, \end{aligned}$$

where $M_{bio}(t) = V_{bio}c_d(t)$ is the drug mass in the bacterial habitat at time t. Assuming that the drug mass available in V_{bio} in each time t is the drug mass $M_s(t)$ (38) released from the polymeric platform, we obtain

$$\begin{aligned} F(c_s(t)) &= \frac{E_{max}M_s(t)^\gamma}{M_{50}^\gamma + M_s(t)^\gamma} \\ &:= F(M_s(t)), \end{aligned}$$

where $M_{50} = V_{bio}c_{50}$ stands for the drug mass leading to half-effect.

As mentioned before, the mathematical model (5), (6), (11), (12), (13) can be used to describe drug release from the polymeric coating of an implant. Once equation (37) is coupled with the drug delivery model it can be used to describe the time evolution of a bacterial population that adheres to the implant causing infection. In this case V_{bio} is the volume of the biofilm developed by bacteria.
Integrating (37) we have

$$N(t) = N(0)e^{\int_0^t(\lambda - F(M_s(\mu)))d\mu}, t \geq 0. \tag{41}$$

Using now Corollary 1, we can compute an upper bound for $N(t)$ in function of the parameters that characterize the drug release system and the drug characteristics.

Proposition 4. *Under the assumptions of Proposition 3 and for $\gamma = 1$, the bacteria density in the biofilm on the polymeric coating satisfies*

$$N(t) \leq N(0)e^{\lambda t - \frac{E_{max}M_d(0)}{M_{50}+M_d(0)}}e^{\frac{E_{max}}{M_{50}+M_d(0)}\sqrt{2|\Omega|}e^{-\frac{1}{2}Qt}\|c_s(0)\|_{L^2(\Omega)}}, t \geq 0. \tag{42}$$

where Q is defined by (27).

Partial derivative	Sign	Monotony of the upper bound of $N(t)$	Previewed behaviour of $N(t)$
$\frac{\partial Q}{\partial D_{eff}(0)}$	$+$	Decreases with $D_{eff}(0)$	Physiological
$\frac{\partial Q}{\partial \bar{\alpha}}$	$+$	Decreases with $\bar{\alpha}$	Physiological
$\frac{\partial Q}{\partial \|v\|_\infty}$	$-$	Increases with $\|v\|_\infty$	Non Physiological
$\frac{\partial Q}{\partial \epsilon_0}$	$+$	Decreases with ϵ	Physiological

TABLE 2. Dependence of the bacterial density on the parameters of the model

Proof: As $M_s(t) \leq M_d(0)$, from (41) we obtain

$$N(t) \leq N(0)e^{\lambda t - \frac{E_{max}}{M_{50}+M_d(0)} \int_0^t M_s(\mu)d\mu}, t \geq 0. \tag{43}$$

The total released drug until time t is given by

$$M_r(t) = \int_0^t M_s(\mu)d\mu = M_d(0) - M_d(t), \tag{44}$$

where $M_d(t)$ denotes the drug mass inside Ω at time t.
Inserting (44) in (43) we get

$$N(t) \leq N(0)e^{\lambda t - \frac{E_{max}M_d(0)}{M_{50}+M_d(0)}} e^{\frac{E_{max}M_d(t)}{M_{50}+M_d(0)}}, t \geq 0. \tag{45}$$

Finally, from Corollary 1 we conclude (42).

■

Considering the behavior of Q described in Table 1 we can deduce for the bacterial density $N(t)$, the monotony properties indicated in Table II. We note that the previewed bacterial density decreases with the porosity ϵ_0 of the implant coating, the diffusion coefficient $D_{eff}(0)$ of the drug at $t = 0$, and dissolution rate α. This point will be addressed is the Conclusions. In Section 4 we illustrate numerically the results in Table 1 and 2.

4. Numerical simulation

4.1. The finite difference method for the coupled problem. In this section we illustrate the behaviour of the coupled model (5), (6), (11), (12),

(13) and (37). The results are obtained considering an IMEX method (implicit-explicit method). Let $H = (\Delta x, \Delta y)$ be a vector of stepsizes for the spatial domain $\Omega = (-1,1)^2$ and let $\overline{\Omega}_H$ be the correspondent spatial grid $\overline{\Omega}_H = \{(x_i, y_j), i = 0, \ldots, M_x, j = 0, \ldots, M_y, x_0 = -1, x_{M_x} = 1, y_0 = -1, y_{M_y} = 1\}$ where $x_i - x_{i-1} = \Delta_x, i = 1, \ldots, M_x$, and $y_j - y_{j-1} = \Delta_y, j = 1, \ldots, M_y$. Let $\Omega_H = \Omega \cap \overline{\Omega}_H$, $\partial\Omega_H = \partial\Omega \cap \overline{\Omega}_H$ and $B_H = B \cap \overline{\Omega}_H$.
Let Δ_H represent the discrete Laplace operator and $\nabla_c = (D_{c,x}, D_{c,y})$, where $D_{c,x}$ and $D_{c,y}$ denote the central finite difference operator that approximate the first order partial derivatives with respect to x and y, respectively. Let D_{+x} and D_{-x} be the second order forward and backward operators defined by

$$D_{+x}u(x_i, y_j) = \frac{1}{2\Delta_x}\Big(- 3u(x_i, y_j) + 4u(x_{i+1}, y_j) - u(x_{i+2}, y_j)\Big)$$

and

$$D_{-x}u(x_i, y_j) = \frac{1}{2\Delta_x}\Big(u(x_{i-2}, y_j) - 4u(x_{i-1}, y_j) + 3u(x_i, y_j)\Big)$$

that approximate the first order partial derivative with respect to x. By D_{+y} and D_{-y} we denote the correspondent operators with respect to y that are defined analogously. These operators will be used to discretize the boundary conditions.
In $[0, T]$ we introduce the uniform mesh

$$\{t_m, m = 0, \ldots, M_t; t_0 = 0, t_{M_t} = T, t_m - t_{m-1} = \Delta t, m = 1, \ldots, M_t\}.$$

By D_{-t} we represent the usual backward finite difference operator

$$D_{-t}u(t_m) = \frac{u(t_m) - u(t_{m-1})}{\Delta t}.$$

By $c^m_{\ell,ij}$, $c^m_{d,ij}$ and $c^m_{s,ij}$ we denote the approximations for $c_\ell(x_i, y_j, t_m)$, $c_d(x_i, y_j, t_m)$ and $c_s(x_i, y_j, t_m)$ defined by the finite difference method:

$$D_{-t}c^m_{\ell,H} + \nabla_c.(vc^m_{\ell,H}) = D_\ell(t_m)\Delta_H c^m_{\ell,H} \text{ in } \Omega_H, \tag{46}$$

$$D_{-t}c^m_{s,H} = -f(c^{m-1}_{s,H}, c^{m-1}_{d,H}, c^m_{\ell,H}) \text{ in } \Omega_H, \tag{47}$$

$$D_{-t}c^m_{s,H} + \nabla_c.(vc^m_{d,H}) = D_{eff}(t_m)\Delta_H c^m_{s,H} + f(c^m_{s,H}, c^{m-1}_{d,H}, c^m_{\ell,H}) \text{ in } \Omega_H, \tag{48}$$

for $m = 1, \ldots, M_t$. System (46), (47), (48) is completed with the initial and boundary conditions

$$c^0_{\ell,H} = 0, c^0_{s,H} = c_s(0), c^0_{d,H} = 0 \text{ in } \Omega_H, \tag{49}$$

$$\begin{array}{l} J^m_{\ell,H}\eta = \beta(c^m_{\ell,H} - c_{ext}) \text{ on } \partial\Omega_H - B_H - \{(-1,1),(1,1)\} \\ J^m_{\ell,H}\eta = 0 \text{ on } B_H - \{(-1,-1),(1,-1)\} \end{array} \tag{50}$$

$$\begin{array}{l} c^m_{d,H} = 0 \text{ on } \partial\Omega_H - B_H - \{(-1,1),(1,1)\} \\ J^m_{d,H}.\eta = 0 \text{ on } B_H - \{(-1,-1),(1,-1)\} \end{array} \tag{51}$$

for $m = 1, \ldots, M_t$.
In (50) $J^m_{\ell,H}$ is defined by

$$J^m_{\ell,H} = -D_\ell(t_m)\nabla_H c^m_{\ell,H} + v c^m_{\ell,H},$$

where $\nabla_H c^m_{\ell,H}(x_i, y_j) = (D_{\pm x}, D_{\pm y}) c^m_{\ell,H}(x_i, y_j)$ with the signal + or − chosen in function of the position on the boundary point (x_i, y_j). The dissolved drug mass flux $J^m_{d,H}$ in (51) is defined analogously.
The discrete drug release problem (46), (47), (48), (49), (50), (51) is coupled with the discrete bacteria problem

$$D_{-t}N^m = (\lambda - F(M^m_s))N^m, m = 0, \ldots, M_t \tag{52}$$

completed with

$$N^0 = N_0. \tag{53}$$

In (52) M^m_s is defined by

$$M^m_s = \sum_{P \in \partial\Omega_H - B_H - \{(\pm 1, \pm 1)\}} \Delta_P J^m_d(P).\eta(P),$$

where $J^m_d(P)$ and $\eta(P)$ denote the dissolved mass flux and the unitary exterior normal to Ω in $P \in \partial\Omega_H - B_H - \{(\pm 1, \pm 1)\}$, respectively. In the definition of M^m_s, Δ_P is equal to Δx (Δ_y) if P is in a part of $\partial\Omega$ parallel to x axis (y axis).

4.2. Numerical results. Except stated otherwise the following set of parameters was considered: $T = 200(h)$, $k_d = 10^{-3}$, $D_{\ell,0} = 10^{-2}$, $D_1 = 10^{-3.5}, D_2 = 10^{-3}(cm^2/h)$, $\epsilon_0 = 10^{-4}$, $\alpha = 10^{-2}(1/h)$ $c_{ext} = 0.7(g/cm^3)$ and $V_{bio} = 0.06(cm^3)$. The distribution of the initial solid drug is defined randomly and is plotted in Figure 2.
To define the spatial grid Ω_H we take $M_x = M_y = 100$ and the temporal grid is defined with $\Delta t = 10^{-3}h$.

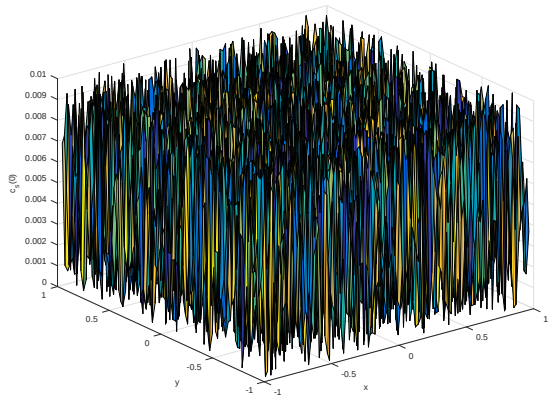

FIGURE 2. Initial solid drug $c_s(0)$.

A global picture of fluid, solid and dissolved drug concentrations in the coating

The concentrations of the fluid and of the solid and dissolved drug are illustrated in Figure 3 for $v = (0, 0)(cm/h)$ and $t = 50, 200(h)$. As the fluid permeates the polymeric coating, the dissolution process occurs, the concentration of the dissolved drug increases and the concentration of the solid drug decreases. After a certain interval of time it permeates the boundary $\partial\Omega - B$ and the concentration of the dissolved drug decreases in the polymeric coating, as can be seen in the plot of $c_d(200)$.

Influence of the drug diffusion coefficient and the fluid convection velocity

The effect of the drug diffusion coefficients, in the polymer and in the fluid filled pores, D_1 and D_2 respectively, is illustrated in Figure 4. We consider their effect on the solid drug mass $M_{sol}(t)$, and on the total released mass in $[0, t]$, $M_r(t)$ (44). As the diffusion coefficients increase, the solid drug mass decreases and the released mass increases. This behaviour is expected because as $D_{eff}(t)$ increases, the passive transport of the dissolved drug increases leading to an increasing of the dissolution of the solid drug.
The influence of the velocity on the drug mass $M_s(t)$, that is released through $\partial\Omega - B$ at each time t, is illustrated in Figure 5. For short times, when the velocity increases, a lower drug mass $M_s(t)$ is observed as a consequence of the increasing of the mass flux. This behaviour is plotted in Figure 5 (left) for $1, 5$ days. After this period, the dependence on the interstitial velocity

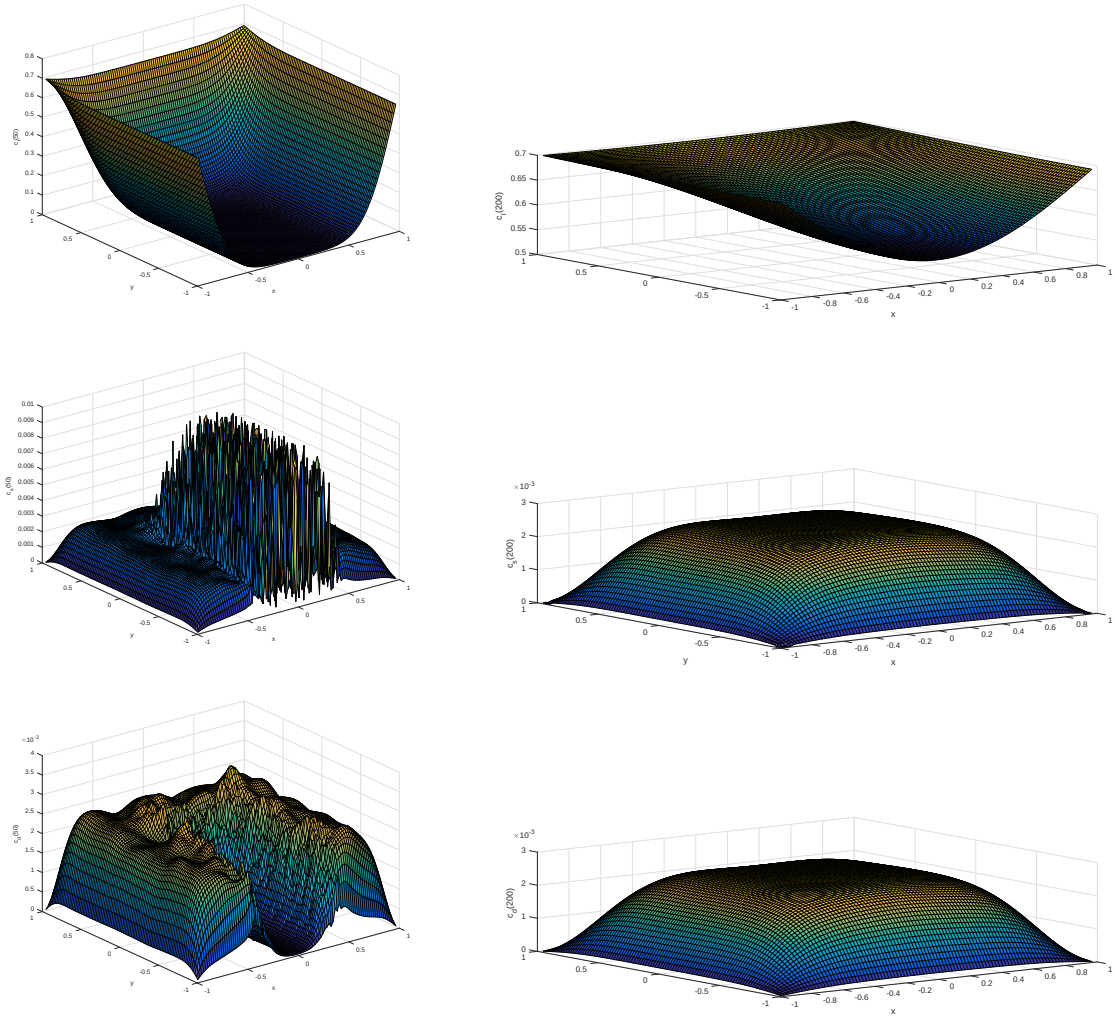

FIGURE 3. Plots of fluid, solid and dissolved drug concentrations at $t = 50, 200(h)$: top row -fluid concentration, middle row- solid drug, bottom row- dissolved drug. The initial distribution of drug is random (Figure 2).

v inverts: for a fixed t the mass $M_s(t)$ that crosses the boundary increases with v. This result is in agreement with ([12]).
The dependence on the velocity v of the total drug released mass in $[0, t]$, $M_r(t)$, is illustrated in Figure 6. $M_r(t)$ has the the same functional dependence on the velocity as $M_s(t)$. The behaviour for short times is not highlighted in Figure 6.

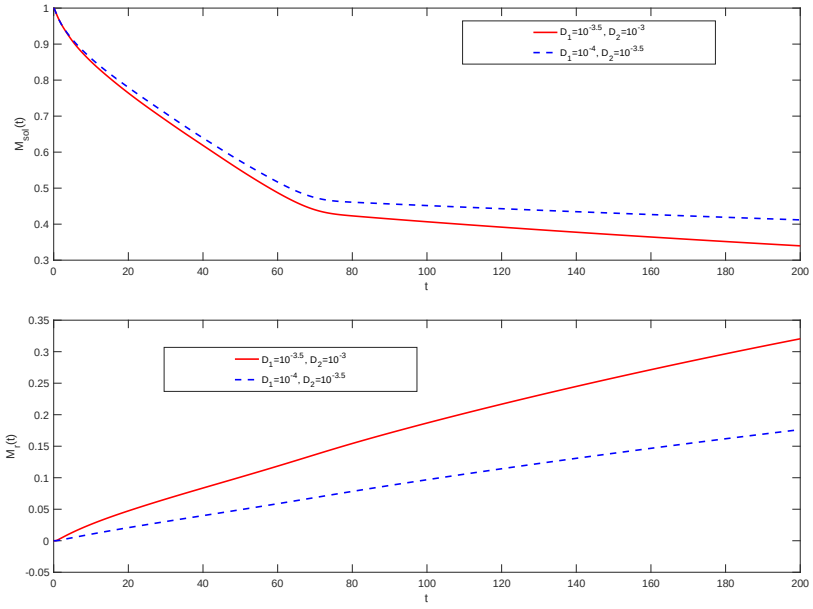

FIGURE 4. Plots of solid mass $M_{sol}(t)$ in the polymer coating and drug released mass $M_r(t)$: top -$M_{sol}(t)$, bottom-$M_r(t)$.

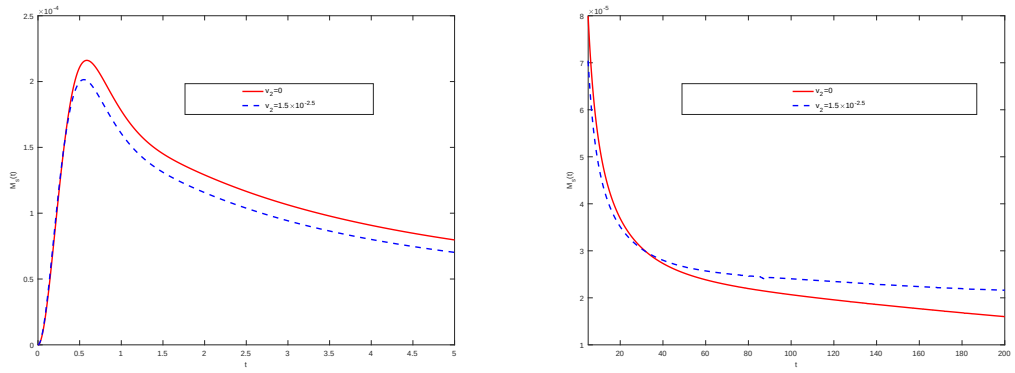

FIGURE 5. Plots of drug masses that permeates the boundary $\partial\Omega - B$ for $v = (0,0)$ and $v = (0, 1.5\times 10^{-2.5})$: left- first 1.5 days, right- last 6.5 days.

Influence of the dissolution rate

We analyse in what follows the effect of the dissolution rate α on the drug release process. We begin by analyzing how the mass of drug inside the polymer depends on α. In Figure 7 we plot the solid drug mass $M_{sol}(t)$ and the dissolved drug mass $M_{dis}(t)$ for different dissolution rates α. As α increases, $M_{sol}(t)$ decreases. The dissolved drug mass $M_{dis}(t)$ presents a two

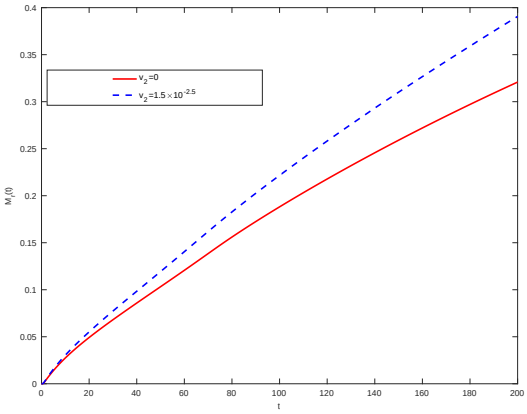

FIGURE 6. Plot of the released drug mass $M_r(t)$ for $v = 0$ and $v = (0, 1.5 \times 10^{-2.5})$.

phase behaviour: for short times it is an increasing function of α; for large times it is a decreasing function of α. This result appears physically sound because, only after an initial period of time, the dissolved drug starts to be released through $\partial\Omega - B$.

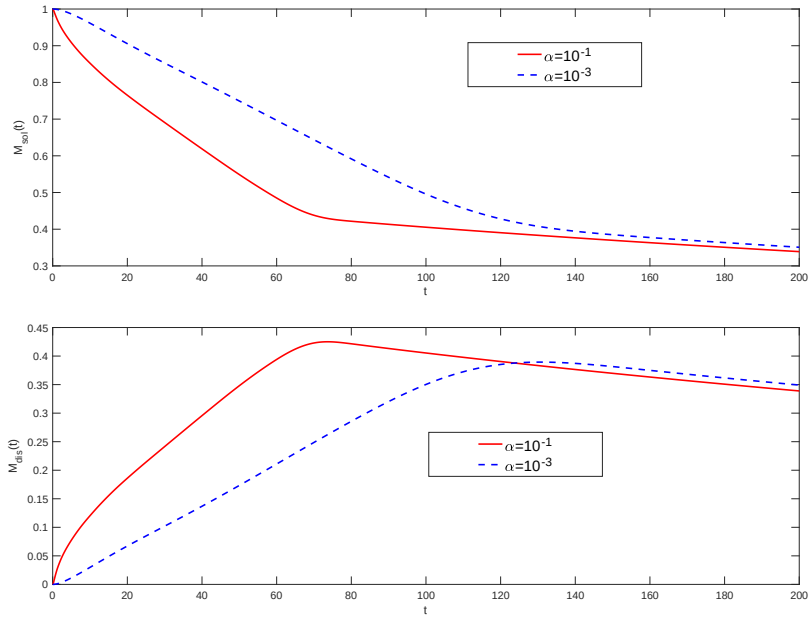

FIGURE 7. Plots of the solid drug mass $M_{sol}(t)$ and dissolved drug mass $M_{dis}(t)$ for different dissolution rates: top-$M_{sol}(t)$, bottom-$M_{dis}(t)$.

Polymeric coating, drug and bacteria

The ultimate aim of the present paper is to study the dependence of bacterial density on the properties of the polymer and the characteristics of the drug. Regarding the properties of the drug, in the bacterial model (37), we illustrate the dependence of $N(t)$ on c_{50} and the cooperation coefficient γ.
We start by analysing the effect of c_{50}. In Figure 8 we exhibit the plot of $M_s(t)$, the mass of drug that crosses the boundary $\partial\Omega - B$ at instant t. We take $c_{50} = 10^{-4.4}, 10^{-2.5}(g/cm^3)$. Let $N_{10^{-4.4}}(t)$ and $N_{10^{-2.5}}(t)$ be the correspondent bacterial densities. The efficacy of the drug decreases with c_{50}. So the simulation in Figure 9 suggests a physiological behaviour, that is $N_{10^{-4.4}}(t) < N_{10^{-2.5}}(t)$, $t \in [0, T]$.
Regarding the cooperation coefficient γ we observe in Figure 9, that for $t > 160$ the population density increases with γ. In $[0, 160[$, for the different γ, the plots are overlapping. However the numerical values obtained show that $N(t)$ decreases with γ. This result can be easily proved from (37).

For $\gamma < 1$ we have in both cases $\lambda - F_{c_{50}}(M_s(t)) < 0$ that leads to $N_{c_{50}}(t) \to 0$ as t increases.

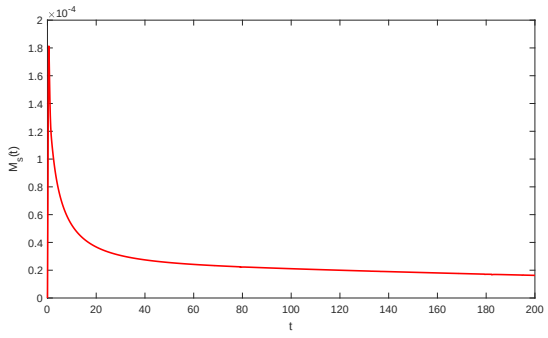

FIGURE 8. Plot of $M_s(t)$ used to obtain the bacteria densities plotted in Figure 9 computed with $\epsilon_0 = 0.1$, $v = 2.5 \times 10^{-2}(0, 1)$, (cm^2/h) ($\|v\| = 2.5 \times 10^{-2}$ (cm^2/h)[11]), $D_1 = 0.5 \times 10^{-3}$, $D_2 = 10^{-2}$ (cm^2/h), $\lambda = 0.56$ $(1/h)$, $N(0) = 10^7(FCU/cm^3)$.

Let us analyze now the influence of the release process. We recall that $D_{eff}(t)$ represents the effective diffusion coefficient of the drug in the porous coating (7). In Figure 10 we exhibit plots of $M_s(t)$ - the mass of drug released at instant t - for different values of D_1, D_2. The result appears physically sound as the largest effective diffusion corresponds to the largest $M_s(t)$. We observe

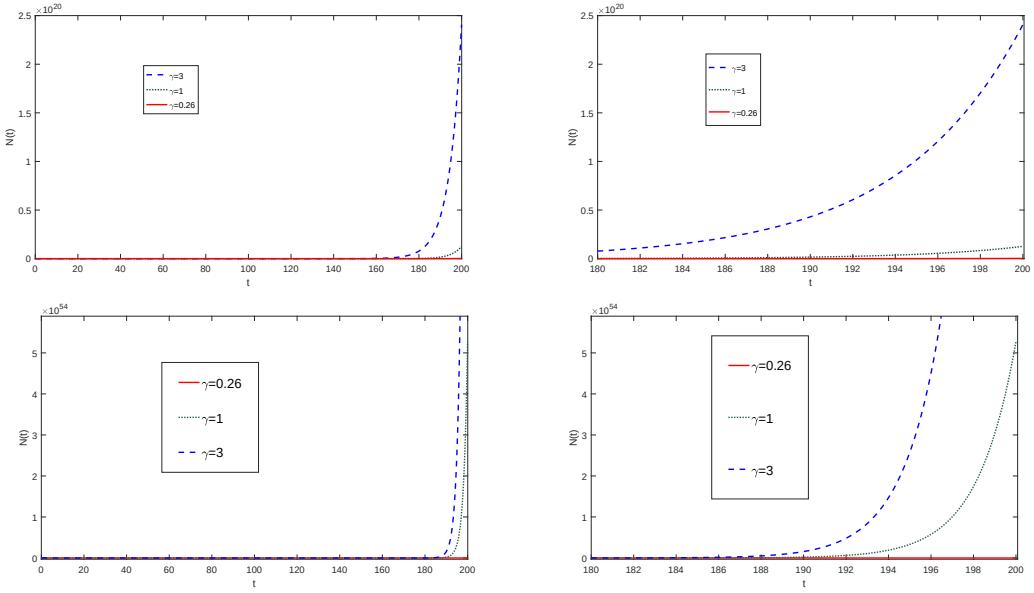

FIGURE 9. Dependence of bacterial density on c_{50}: top left-$N(t)$ for $c_{50} = 10^{-4.4}$, top right-zoom of the left picture, bottom left - $N(t)$ for $c_{50} = 10^{-2.5}$, bottom right-zoom of the left picture .

an initial burst followed by a period of steep decrease and a period of steady release.

In Figure 11 we illustrate the effect of $D_{eff}(t)$ on bacterial density $N(t)$ for $c_{50} = 5.1 \times 10^{-6}$ (g/cm^3). By $D_{eff,1}(t)$ we denote the effective diffusion coefficient for $D_1 = 0.5 \times 10^{-4}$, $D_2 = 0.5 \times 10^{-3.5}$ and by $D_{eff,2}(t)$ the effective diffusion coefficient obtained for $D_1 = 0.5 \times 10^{-3.5}$, $D_2 = 0.5 \times 10^{-3}$. We use the notations $N_{D_{eff}}(t)$ and $F_{D_{eff}}(M_s(t))$ to take into account the dependence of $N(t)$ and $F(M_s(t))$ on D_{eff}. We highlight two aspects in Figure 11. Firstly the fact that the bacterial population is not eliminated when the drug has effective coefficient $D_{eff,1}(t)$. From an analytical point of view, this fact is easily explained because $F_{D_{eff,1}}(M_s(t)) < 0$, for $t < \tilde{t}$, for a certain time $\tilde{t}$, but $F_{D_{eff,1}}(M_s(t)) > 0$, for $t > \tilde{t}$. This means that $N_{D_{eff,1}}(t)$ decreases in $(0, \tilde{t})$ and increases in $(\tilde{t}, 200)$. The second aspect regards the comparison of the bacterial populations corresponding to $D_{eff,1}$ and $D_{eff,2}$. As expected the largest population corresponds to $D_{eff,1}(t)$.

The simulations in Figure 11 suggest that if the effective diffusion $D_{eff}(t)$ is not large enough than the antibacterial fight can be ineffective. From (7), $D_{eff}(t)$ depends on the interplay between the characteristics of the drug and the properties of the material, namely its porosity. The illustration in Figure

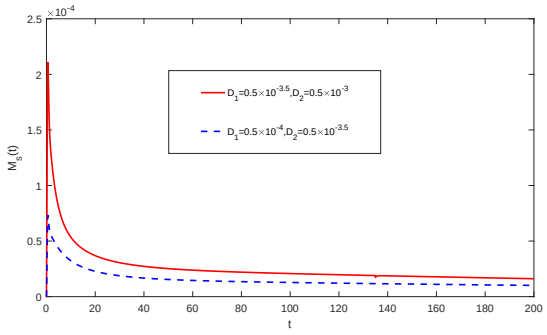

FIGURE 10. Plots of $M_s(t)$ used to obtain bacterial densities plotted, in Figure 11, computed with $\epsilon_0 = 0.1$, $v = 2.5 \times 10^{-2}(0,1)$, (cm^2/h) $(\|v\| = 2.5 \times 10^{-2}$ $(cm^2/h)[11])$, $c_{50} = 5.1^{\times}10^{-6}$ (g/cm^3), $\lambda = 0.56$ $(1/h)$, $N(0) = 10^7(FCU/cm^3)$.

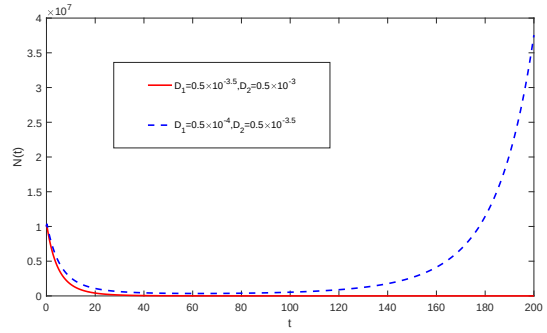

FIGURE 11. Plots of bacterial densities when the effective diffusion coefficient $D_{eff}(t)$ increases. If $D_{eff}(t)$ is not large enough the bacterial density explodes.

11 shed light on the the fact that a successful fight, against an opportunistic bacterial population, depends on a compromise between drug characteristics and polymeric platform properties.

We illustrate now the influence of the coating porosity. In Figure 12 we exhibit the behaviour of $N(t)$ when we change the initial porosity. We use the notation $N_{\epsilon_0}(t)$ to highlight the dependence of $N(t)$ on ϵ_0. We observe that $N_{10^{-1}}(t) \leq N_{10^{-2}}(t)$, for all t. In fact, as ϵ_0 increases, the effective diffusion coefficient $D_{eff}(t)$ also increases.

5. Conclusions

Biocompatible polymers play a crucial role in controlled drug delivery technology because they provide platforms that can release therapeutic agents to

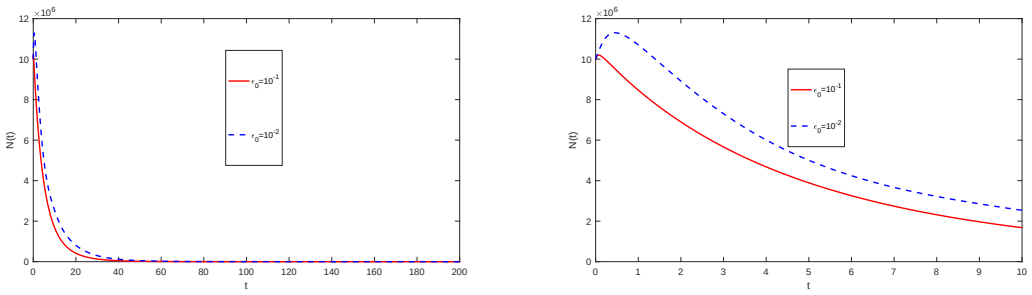

FIGURE 12. Plots of bacterial densities when the initial porosity increases (left) and its zoom (right), computed with $D_1 = 0.5 \times 10^{-3}$, $D_2 = 10^{-2}$ (cm^2/h) and $c_{50} = 5.1 \times 10^{-6}$ (g/cm^3).

targeted tissues or organs during long periods. Medical implants are sometimes colonized by bacteria forming a biofilm at their surface and leading to infectious process that are very difficult to treat effectively. Often, the only treatment for biofilm infections is to remove the implant, fight the infection with antibiotics, and replace the implant, which represents a damaging, risky and expensive procedure. An alternative used nowadays is to use implants coated with a porous polymer layer where antibacterial agents are dispersed. An important type of implants are metallic orthopedic prosthesis coated with drug eluting polymeric layers ([2, 6, 8, 14, 16, 18, 23, 24, 25, 26]).
The motivation of this paper is to model the release of drug from a polymeric platform and its simultaneous action in combating opportunistic infection by pathogens. More exactly we address the problem of predicting the evolution of a bacterial population from the parameters that characterize the polymeric platform and the pharmacokinetics of the drug. To describe the whole process we propose a system of partial differential equations coupled with an ordinary differential equation. The system of PDE's governs the drug release from a biodegradable polymer coating and the ODE is used to describe the time evolution of a bacterial population attached to the surface.
At the best of our knowledge the paper contains original contributions. Regarding theoretical results we mention:

(a) The type of coupling between the system of PDE's and the ODE made by an integral that represents the mass of drug released at instant t (38);
(b) A "quasi-sharp" estimate of the bacterial density $N(t)$, in the sense that the upper bound obtained exhibits a physiological dependence

on the parameters of the model, giving information on how to control the bacterial density (Tables 1 and 2). This "quasi-sharpness" points a way of bridging the gap between theoretical analysis and practical outcomes.

From an applied point of view, the simulation outcomes allow us to shed light on different aspects of bacterial growth:

(a) The influence of interstitial velocity on drug release: "The fasten the flow rate, higher concentrations are released"(see [12])(Figure 6);
(b) The influence of effective diffusion, in the polymeric layer, on the mass of drug released in the bacterial film: the larger the effective density, the smaller the bacterial population (Figure 11). A successful fight, depends not only on drug properties but also on material platform properties;
(c) The influence of polymer porosity on the bacterial density (Figure 12).

Regarding this last point a clarification is due. The result in Figure 12 states that the bacterial density decreases with porosity. In the scenario of Hill model (37) this has a simple explanation: the larger the porosity, the greater the mass released at instant t, $M_s(t)$, and consequently the smaller is the bacterial population. However, as mentioned in [1],"... the introduction of pores inherently increases the surface roughness and also the risk of bacterial adherence". This paper contains an exploratory approach and further studies on the topic should include an improvement of Hill's model namely inserting a functional dependence of the growth rate λ (37) on the porosity. This functional dependence should be based on laboratorial experiments.
Finally we observe that macroscopic models, like the Hill model, have many advantages due to the fact that they can provide global pictures of the process. However for situations where only a few bacterial cells exist or survive the therapeutic agent, the coupling of the PDE's system with agent based models should deserve attention.

6. Acknowledgements

The first and fourth authors were supported by the project *NEXT.parts - Next- generation of advanced hybrid parts*, funded by EU's Horizon 2020 science programme (Portugal 2020, COMPETE 2020).

The second and last authors were supported by the project *NEXT.parts - Next- generation of advanced hybrid parts*, and by Centro de Matemática

da Universidade de Coimbra—UID/MAT/00324/2013, funded by the Portuguese Government through FCT/MCTES and co-funded by the European Regional Development Fund through the Partnership Agreement PT2020.

7. Appendix

Proof of Proposition 1: To establish the existence of $\mu \neq 0$ such that (19) holds we start by proving the existence of $\epsilon \neq 0$ such that

$$P(\epsilon) := \|v(t)\|_\infty^2 \epsilon^2 - 2\epsilon D_{eff}(t) + C_P^2 < 0. \tag{54}$$

The zeros of the polynomial $P(\epsilon)$ are defined by

$$\epsilon_\pm = \frac{1}{\|v\|_\infty^2}\Big(D_{eff}(t) \pm \sqrt{D_{eff}^2 - C_P^2\|v\|_\infty^2}\Big),$$

then the positive the zeros of $\|v(t)\|_\infty^2\mu^4 - 2\mu^2 D_{eff}(t) + C_P^2$ are defined by (18). Consequently, for $\mu \in]\mu_-, \mu_+[$, where $\mu_- > 0$, we have (19).
We remark that

$$\frac{\partial \mu_-^2}{\partial t} \leq 0, \; \frac{\partial \mu_+^2}{\partial t} \geq 0, \; t \geq 0,$$

and then μ_- decreases with t and μ_+ increases with t. In order to select an interval time independent where $\|v(t)\|_\infty^2\mu^4 - 2\mu^2 D_{eff}(t) + C_P^2 < 0$, for all t, we use the monotonicity of $\mu_\pm(t)$. It is easy conclude that for $\mu \in]\mu_-(0), \mu_+(0)[$ we have (19).

■

References

[1] A. Braem, L. Van Mellaert, D. Hofmans, E. De Waelheyns, J. Anné, J. Schrooten, J. Vleugels, Bacterial colonisation of porous titanium coatings for orthopaedic implant applications -Effect of surface roughness and porosity, Powder Metallurgy, 56, 267, 2013.

[2] A. de Breij, M. Riool, P.Kwakman, L. de Boer, R.A. Cordfunke, J.W. Drijfhout, O. Cohend, N. Emanuel, S.A.J. Zaat, P.H. Nibbering, T.F. Moriarty, Prevention of Staphylococcus aureus biomaterial-associated infections using a polymer-lipid coating containing the antimicrobial peptide OP-145, Journal of Controlled Release, 222 1-8, 2016.

[3] J.A. Ferreira, M. Grassi, E. Gudiño, P. de Oliveira, A 3D model for mechanistic control drug release, SIAM Journal on Applied Mathematics, 74, 620–633, 2014.

[4] J.A. Ferreira, L. Gonçalves, J. Naghipoor, P. de Oliveira, T. Rabczuk, The influence of atherosclerotic plaques on the pharmacokinetics of a drug eluted from bioabsorbable stents, Journal of Mathematical Bioscience, 283, 71–83, 2017.

[5] J.A. Ferreira, M. Grassi, P. de Oliveira, G. Romanazzi, Drug release from viscoelastic swelling polymeric platforms, IAM Journal on Applied Mathematics, 78, 1378–1401, 2018.

[6] J. Gallo, M. Holinka, C. S. Moucha, Antibacterial surface treatment for orthopaedic implants, International Journal of Molecular Sciences, 15, 13849–13880, 2014.

[7] M. Gimeno, P. Pinczowski, M. Pérez, A. Giorello, M.A. MartÃnez, J. Santamaría, M. Arruebo, L. Luján, A controlled antibiotic release system to prevent orthopedic-implant associated infections: an *in vitro* study, European Journal of Pharmaceutics and Biopharmaceutics, 96, 264–271, 2015.

[8] S. Goodman, Z. Yao, M. Keeney, F. Yang, The future of biologic coatings for orthopaedic implants, Biomaterials, 34, 3174–3183, 2013

[9] S. Goutellea, M. Maurinc, F. Rougierb, X. Barbautb, L. Bourguignona, M. Ducherb, P. Mairea, The Hill equation: a review of its capabilities in pharmacological modelling, Fundamental & Clinical Pharmacology, 22, 633–648, 2008.

[10] M. Grassi, G. Grassi, Mathematical modelling and controlled drug delivery: matrix systems, Current Drug Delivery, 2, 97–116, 2005.

[11] W. Yao, Y. Li, G. Ding, Interstitial fluid flow: the mechanical environment of cells and foundation of meridians, Evidence-Based Complementary and Alternative Medicine, 2012, Article ID 853516, 9 pages, 2012.

[12] T. Kumeria, K. Gulati, A. Santos, D. Losic, Real-time and in situ drug release monitoring from nanoporous implants under dynamic flow conditions by reflectometric interference spectroscopy, ACS Applied Materials & Interfaces, 5, 5436–5442, 2013

[13] S. McGinty, S. McKee, C. McCormick, Release mechanism and parameter estimation in drug-eluting stent systems: analytical solutions of drug release and tissue transport, Mathematical Medicine and Biology, 32, 163–186, 2015.

[14] T. Moriarty, R. Kuehl, T. Coenye, W-J. Metsemakers, M. Morgenstern, E. Schwarz, M. Rioo, S. Zaat, N. Khana, S. KatesR. Richards, Orthopaedic device-related infection: current and future interventions for improved prevention and treatment, EFORTS Open Reviews, 1, 89–99, 2017.

[15] J. Naghipoor, J.A. Ferreira, P. de Oliveira, T. Rabczuk, Tuning polymeric and drug properties in a drug eluting stent: anumerical study, Applied Mathematical Modeling, 40, 8067–8086, 2016.

[16] C. Pan, Z. Zhou, X. Yu, Coatings as the useful drug delivery system for the prevention of implant-related, Journal of Orthopaedic Surgery and Research, 13, 220, 2018. infections

[17] Y.S. Park, J.Y. Cho, S.J. Lee, C. Hwang, Modified titanium implant as a gateway to the human body: the implant mediated drug delivery system, BioMed Research International, 2014, Article ID 801358, 6 pages, 2014.

[18] M. Prakasam, J. Locs, K. Salma-Ancane, D. Loca, A. Largeteau, L. Berzina-Cimdina, Biodegradable materials and metallic implants - a review, Jornal of Functional Biomaterial, 8, 44, 2017.

[19] L. Pisani, Simple Expression for the tortuosity of porous media, Transport in Porous Media, 88, 193–203, 2011.

[20] K. Poelstra, N. Barekzi, M. Rediske, A. Felts, J. Slunt, D. Grainger, Prophylactic treatment of gram-positive and gram-negative abdominal implant infections using locally delivered polyclonal antibodies, Journal of Biomedical Materials Research Part A, 60, 206–2015, 2002.

[21] J. Siepmann, F. Siepmann, Mathematical modeling of drug dissolution, International Journal of Pharmaceutics, 453, 12–24, 2013.

[22] Z. Song, L. Borgwardt, N. Høiby, H. Wu,T. S Sørensen, A. Borgwardt, Prosthesis infections after orthopedic joint replacement: the possible role of bacterial biofilms, Orthopedic Reviews, 5, 65–71, 2013.

[23] C. Strobel, N. Bormann, A. Kadow-Romacker, G. Schmidmaier, B. Wildemann, Sequential release kinetics of two (gentamicin and BMP-2) or three (gentamicin,IGF-I and BMP-2) substances from a one-component polymeric coating on implants, Journal of Controlled Release, 15, 37–45, 2011.
[24] V.J. Suardi, D. A. Bichara, S. J. J. Kwok, A. A. Freiberg, H. Rubash, H. Malchau, S. H. Yun, O. K. Muratoglu, E. Oral, A fully functional drug-eluting joint implant, Nature Biomedical Engineering 1, Article number: 0080, 2017, doi: $10.1038/s41551 - 017 - 0080$.
[25] E. Tobin, Recent coating developments for combination devices in orthopedic and dental applications: a literature review, Advanced Drug Delivery Reviews, 112, 88–100, 2017.
[26] B. Zhang, D. Myers, G. Wallace, M. Brandt, P. Choong, Bioactive coatings for orthopaedic implants-recent trends in development of implant coatings, International Journal of Molecular Sciences, 15, 11878–11921, 2014.
[27] X. Zhu, R. Braatz, A mechanistic model for drug release in PLGA biodegradable stent coatings coupled with polymer degradation and erosion, Journal of Biomedical Materials Research Part A, 103, 2269–2279, 2015.

Raquel Bernardes
Department of Mathematics, University of Coimbra, Apartado 3008, EC Santa Cruz, 3001-501 Coimbra, Portugal

E-mail address: raquelvbernardes@hotmail.com

J.A. Ferreira
CMUC, Department of Mathematics, University of Coimbra, Apartado 3008, EC Santa Cruz, 3001-501 Coimbra, Portugal

E-mail address: ferreira@mat.uc.pt
URL: http://www.mat.uc.pt/~ferreira

M. Grassi
Department of Engineering and Architecture, University of Trieste, Trieste, Italy

E-mail address: MARIO.GRASSI@dia.units.it

M. Nhangumbe
Department of Mathematics, University of Coimbra, Apartado 3008, EC Santa Cruz, 3001-501 Coimbra, Portugal

E-mail address: meloacacio@hotmail.com

Paula de Oliveira
CMUC,Department of Mathematics, University of Coimbra, Apartado 3008, EC Santa Cruz, 3001-501 Coimbra, Portugal

E-mail address: polivei@mat.uc.pt
URL: http://www.mat.uc.pt/~poliveir/